Projected Pinhole Diffraction

A Senior Project

By

David Moore

Advisor, Dr. Glen Gillen

Department of Physics, California Polytechnic University SLO

June 8, 2011

Contents

List of Tables

List of Figures

Abstract

The goal of this experiment was to observe the effects of passing light through a pinhole, more specifically, to observe the interference and diffraction that occurs due to the pinhole and to successfully achieve CCD camera recording of a projected diffraction pattern from a pinhole. This experiment involved the diffraction of a laser incident upon a 100-μm diameter circular aperture. The diffraction pattern is then projected using a 100-mm focal length plano-convex lens. The lens allows for the pattern to be magnified and stretched a few focal lengths past the lens where it can be then viewed using a CCD camera in an optics-free region.

1. Introduction

The main point of interest in this experiment is the diffraction that occurs at the pinhole. Diffraction, according to the authors of *Introduction to Optics,* is "any deviation from geometrical optics that results from the obstruction of a wavefront of light" [1]. Laser light incident upon a small pinhole would form an interference pattern. According to *The Physics of Vibrations and Waves,* by H. J. Pain, "Diffraction is classified as Fraunhofer or Fresnel. In Fraunhofer diffraction the pattern is formed at such as distance from the diffraction system that the waves generating the pattern may be considered as plane" [2]. The diffraction that we will be looking at in this experiment can easily be confused to be Fraunhofer diffraction, since the CCD camera that will be detecting the interference due to the diffraction will be far enough away from the various slits used. Basically, the improper line of thinking is that the distance to the point of interest is much bigger than the aperture size (the slit width or in this case, the diameter of the pinhole). *However*, the diffraction pattern is only far away from the pinhole because it is projected away from the pinhole. This type of diffraction is Fresnel diffraction; it is right in front of the aperture.

2. Theory

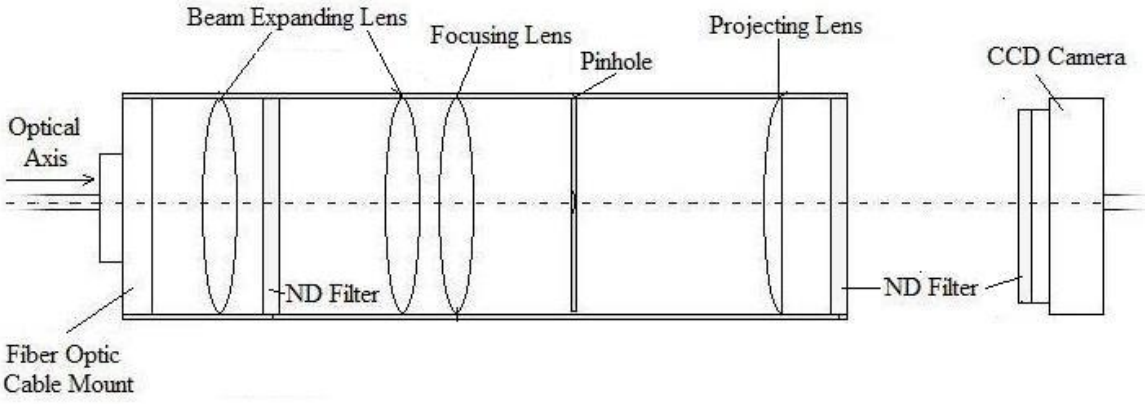

Figure 1. Theoretical set up for projected pinhole diffraction.

2.1 Beam Expander

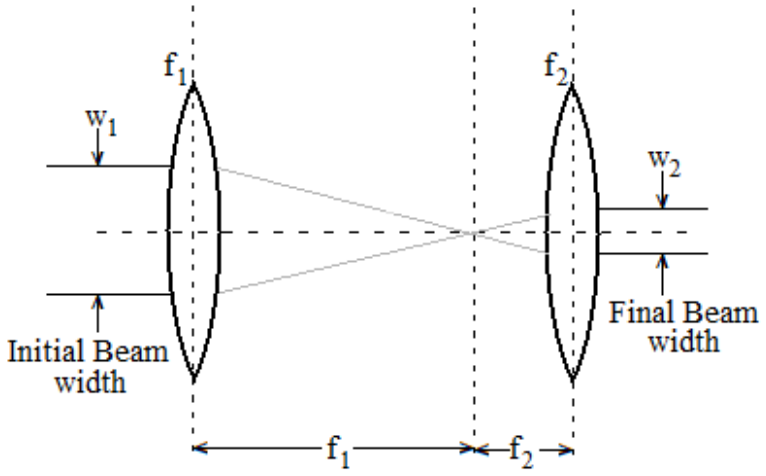

Figure 2. Theoretical setup for the beam expanding lens system from Figure 1.

The laser light that exits the fiber optic cable was then sent through a series of two lenses with the purpose of expanding the beam diameter. Figure 2 shows how a beam expander should be used to change the size of the laser beam width for our experiment. The beam expander was used in reverse to shrink the width of the beam. The width of the output beam of light w_2 can be expressed as

$$w_2 = \frac{f_2}{f_1} w_1 \ , \qquad (1)$$

where w_1 is the original beam width, f_1 is the focal length of the first biconvex lens (where $f_1 > f_2$), and f_2 is the focal length of the second biconvex lens.

2.2 The Purpose of the Focusing Lens

The use of the beam expander to shrink the beam was a critical for the quality of the beam. The beam was too big for the pinhole aperture, which has only a 50-μm radius! In order for proper diffraction to occur, the light hitting the pinhole needed to be plane waves coming at the pinhole with the waves normal to the surface of the pinhole aperture. One way of accomplishing this was to use a lens to focus the light down, at to have the pinhole be at the focal spot of the lens where the light has the smallest waist. At this point the light waves are planar and normal to the surface of the aperture!

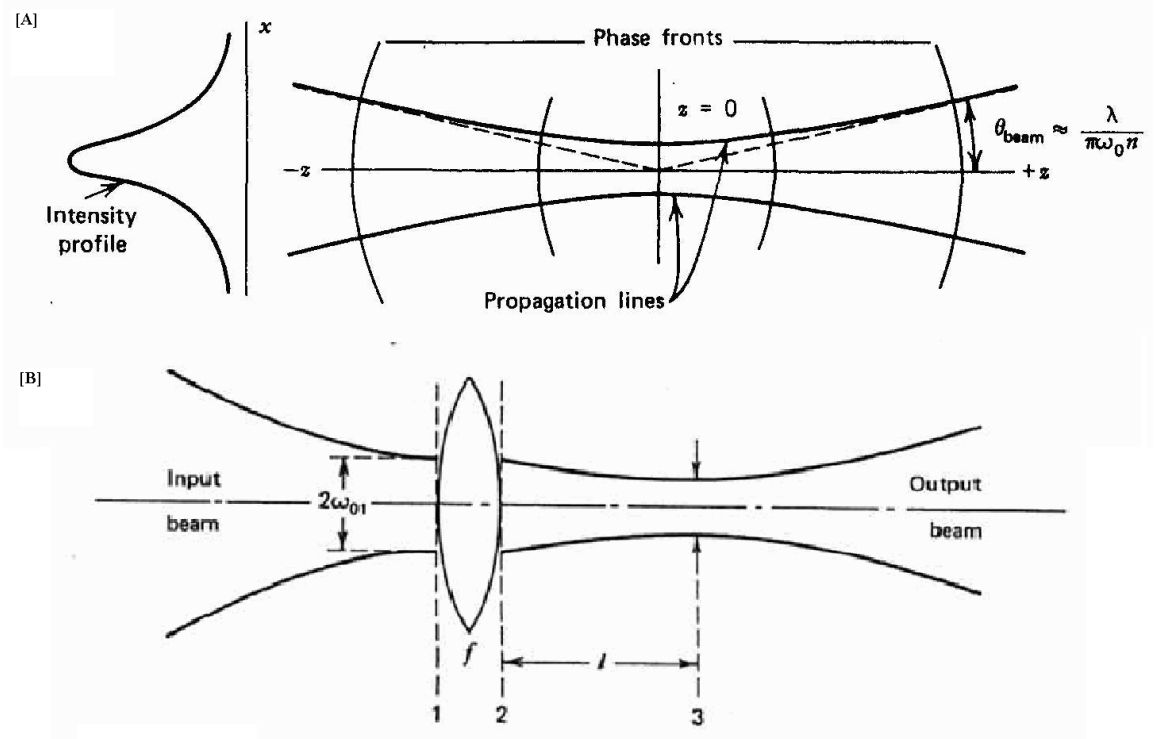

Figure 3. (A) Phase fronts of a focused beam going from converging to diverging at the focal plane. (B) Focusing of a Gaussian Beam. --From cited source [3].

Figure 3 shows how a Gaussian beam interacts with a focusing lens. The first caveat here is that the intensity profile of our beam is not Gaussian, it is more like a top hat (see figure 9 for comparison of our beam profile to a Gaussian beam profile). So this is only a model of how the beam should be acting ideally. We can see in Figure 3A that the phase fronts of the focusing beam change as the beam approaches the focal plane. The phase fronts are either converging or diverging (converging when approaching the focal plane, diverging when leaving the focal plane) but at the focal plane the phase front is neither! The phase front becomes planar, where before the phase fronts were thought to be fronts of a spherical wave (where the sphere has a radius R). However *at* the focal plane the radius of the spherical wave front goes to infinity, in other words, the focal plane has planar waves of light, neither converging nor diverging.

2.3 Pinhole Placement

The focal plane is the desired location to place our pinhole aperture. As was briefly mentioned before; in order for proper diffraction to occur at the pinhole, any light hitting the pinhole would need to be plane waves to be normal to the surface of the pinhole aperture in order for the experimental results to match what is theoretically predicted and desired.

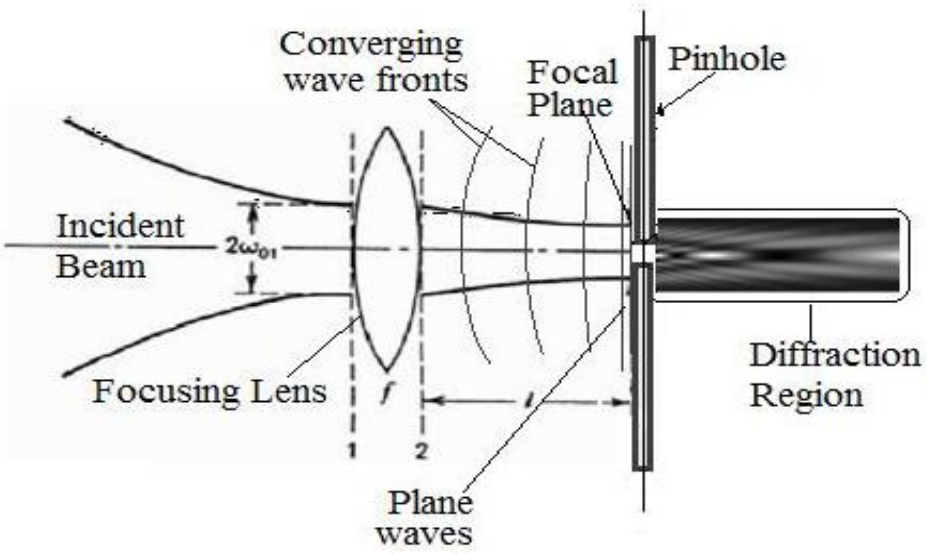

Figure 4. Plane Waves at the focal plane of a focusing lens --allow for proper pinhole diffraction.

Figure 4 shows the proper alignment of the pinhole so that the incoming light can properly diffract; the light hitting the pinhole is planar. There is another reason the focal plane is the ideal place to align the pinhole aperture. The intensity of the light is the greatest at the focal plane. If we were to point the laser beam onto the pinhole only a small fraction of the intensity would go through the pinhole. Focusing the light is a solution to the loss of intensity. All of the intensity of the beam in the focused beam spot. In this way a higher percentage of the light beam goes through the pinhole so there is more intensity in the diffraction pattern. In general, a more intense diffraction pattern is an easier to see and more defined diffraction pattern.

Another great reason to place the pinhole at the focal plane of the focusing lens is to select a desired fraction of the Gaussian beam. Ideally, to duplicate a pseudo-plane wave one should have the one aperture 3 to 5 times smaller than the beam.

2.4 The Pinhole

The diffraction in front of the pinhole is actually changing as the light travels along the optical axis through and away from the pinhole. The diffraction pattern is so close to the pinhole aperture that it would be near impossible to examine this pattern with a CCD camera at its source. The pinhole would simply get in the way. For this reason, we projected the near-field diffraction pattern using a lens. The diffraction pattern could then be viewed easily with no obstruction limiting our view.

Figure 7 shows the theoretical setup for projecting near-field diffraction patterns. The projection lens, with focal length *f*, is placed a distance *L* away from the pinhole aperture, where $L > f$. This accomplishes the goal of projecting the diffraction pattern from just beyond the pinhole to an optics-free region. Figure 7 was made possible to theorize by the means of Fresnel approximation for diffracted fields at a point in the near-field diffraction region. This Fresnel approximation can be expressed in cylindrical coordinates as

$$E_1(r_1, z_1) = \frac{ke^{ikz_1}}{iz_1} \exp\left[i\frac{kr_1{}^2}{2z_1}\right] x \int_0^a E_{z_0} J_0\left(\frac{kr_0 r_1}{z_1}\right) \exp\left[i\frac{kr_0{}^2}{2z_1}\right] r_0\, dr_0 \quad , \qquad (2)$$

where k is the wave number, r_1 is the location of the point of interest in the diffraction region, r_0 is an integration point in the pinhole, and E_{z0} is the distribution of the incident electric field within the open area of the pinhole. Since the laser light that will be incident on the pinhole will be focused down, the light will be plane waves so this E_{z0} can be assumed to be constant. Finally, J_0 is a Bessel function of the first kind with order zero [4]. Unfortunately, a detailed explanation of the physics behind this Fresnel approximation is beyond the scope of this paper

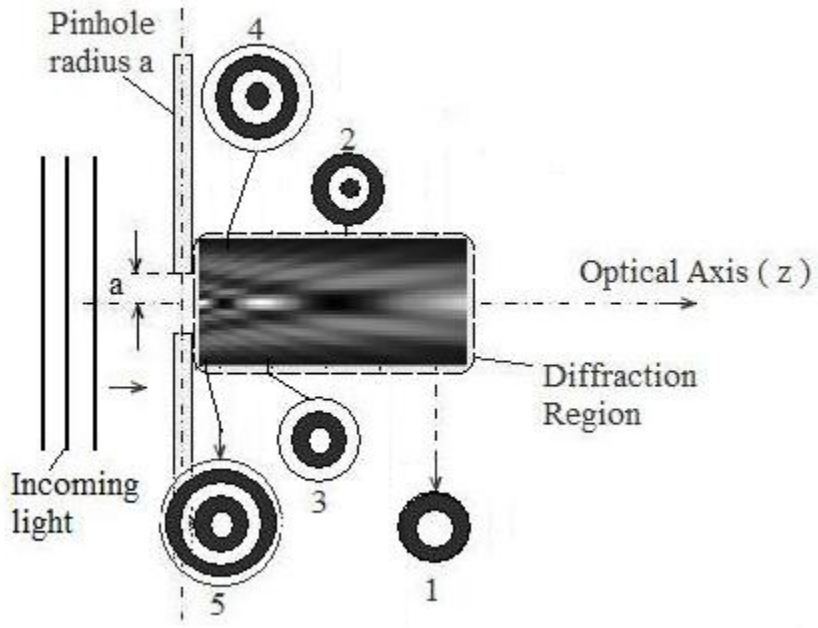

Figure 5. Exaggerated diffraction region just beyond pinhole radius a, with 2-D slices of key diffraction images.

Figure 5 shows an exaggerated look at what is happening immediately beyond the pinhole. The near-field diffraction has a pattern that changes as a function of axial distance away from the pinhole. Images 1-5 within figure 5 are two dimensional slices of the diffraction pattern at different indicated positions. Figure 5 shows how the diffraction pattern progresses in space, actual diffraction images collected with this experimental set up in the data and analysis section of this report.

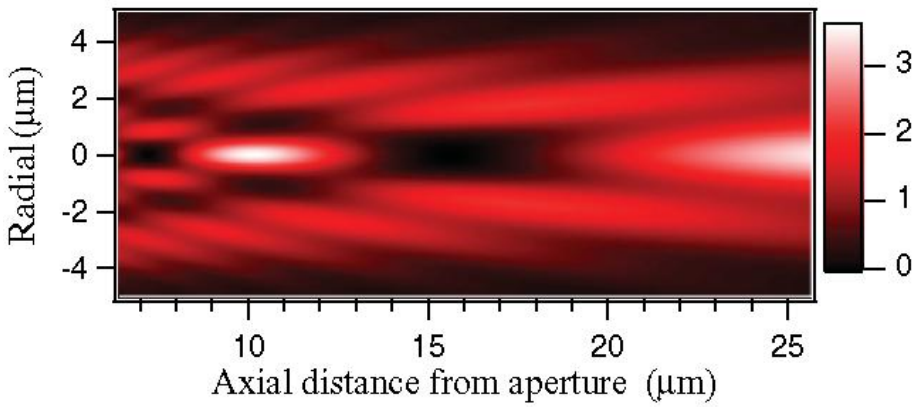

Figure 6. Example Intensity pattern of light diffracting just beyond the pinhole as a function of axial distance

Figure 6 shows just how the diffraction pattern changes for the near-field just beyond the pinhole aperture. The figure is a continuous image of the morphing intensity pattern. This image is merely a two-dimensional rendering of the diffraction that occurs at the pinhole. In reality, this 2-D image is rotated along the optical axis and is a cylindrically-symmetric pattern made up of rings of differing intensities. In this way, a two-dimensional slice of the pattern at a particular axial distance would give you a particular diffraction "image slice" (such as the 2-D slices seen in figure 5 and figure 7 and figure 11).

2.5 Pattern Projection

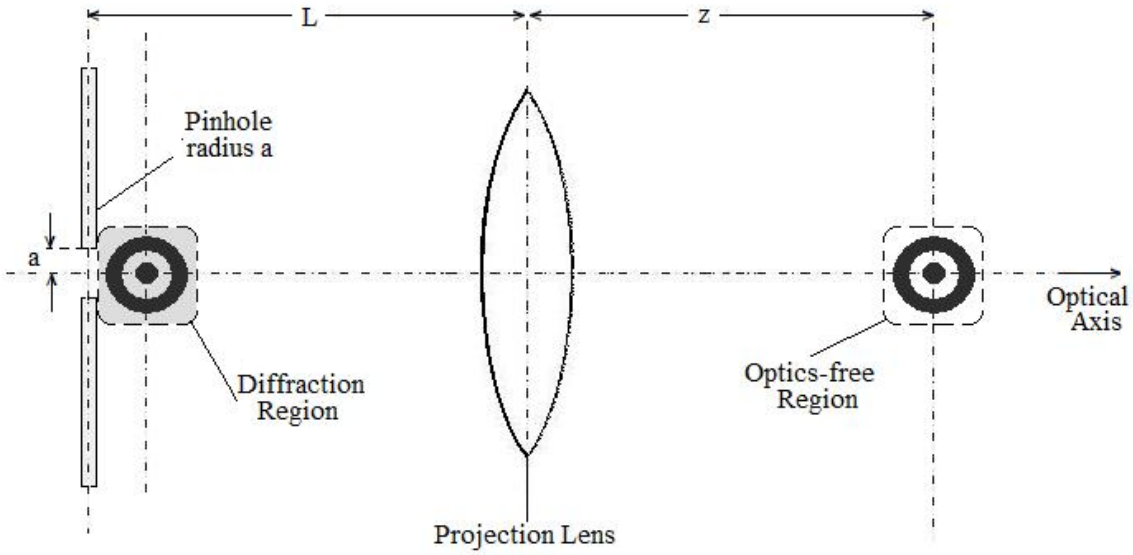

Figure 7. Theoretical setup for projecting near-field diffraction patterns to an optics-free region

The diffraction pattern immediately in front of the pinhole may also be referred to as the near-field diffraction pattern. In figure 7 the diffraction region contains a small set of rings. These rings are not positioned as they would be seen in real three-dimensional space. Rather, these rings are a single two-dimensional slice of one part of the near-field diffraction pattern. The near-field diffraction pattern actually extends for a short distance

nearby the exit of the pinhole and this entire pattern can be projected by a lens. This pattern can then be imaged one slice at a time by using a movable mounted CCD camera that can collect and store images.

The variables seen in figure 7, relate to the projection of the diffraction pattern and can be represented as

$$\frac{1}{f} = \frac{1}{\left(L - \frac{a^2}{n\lambda}\right)} + \frac{1}{z}. \qquad (3)$$

Here, we see that equation (3) is written in a very familiar style, similar to the thin lens equation in geometric optics. Where *f* is the focal length of the projection lens, *L* is the distance from the lens to the pinhole aperture, *a* is the aperture radius, λ is the wavelength of the light, *z* is the distance from the lens to the projected diffraction pattern. Finally, *n* is a nonzero integer. On-axis maxima correspond to when *n* is an odd integer, minima when *n* is an even integer.

For two on-axis locations of interest for this experiment, a value of $n = 2$ corresponds to the projection of the primary blue-detuned trap (donut shaped pattern in figure 12A), and a value of $n = 3$ corresponds to the projection of the primary red-detuned trap (target shaped pattern in figure 12B) [5]. Notice the order of the *n* values 1-5 in figure 5.

3. Experimental Setup

Equipment List:

- Thorlabs CCD camera (make and model)
- Thorlabs Lenses
- Thorlabs 100mm Pinhole
- 780nm Diode Laser (make and model)
- Fiber optic cable
- Fiber optic cable mount
- Various ND filters
- Various optical mounts

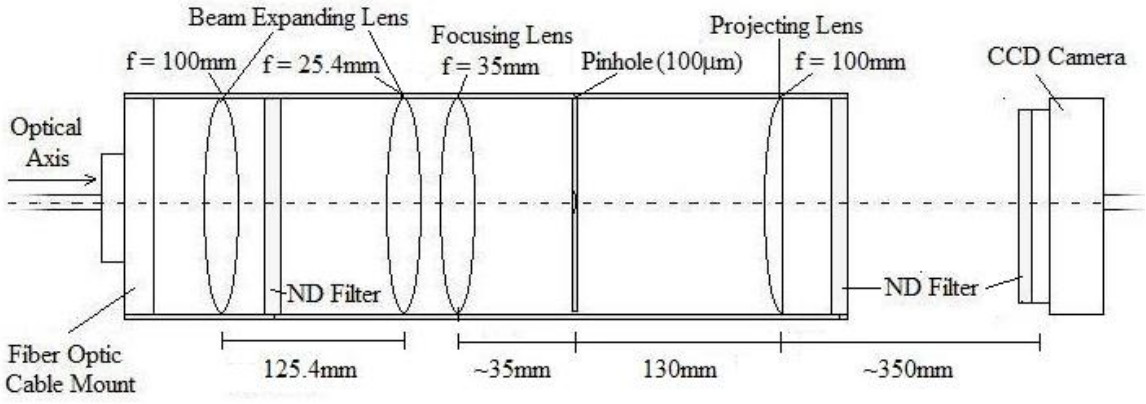

Figure 8. Experimental set up for projected pinhole diffraction

3.1 Laser and fiber optic cable

The goal here was to project a three-dimensional diffraction pattern from in front of a pinhole, to a optical instrument-free zone. The starting point was the type of laser. The laser used in this lab was a diode laser with a variable output power source at a wavelength of 780 nanometers. This wavelength of light is on the fringe of the visible spectrum, so despite the fact that the laser output power was around 45 mW, the laser was still so faint that the naked eye had trouble seeing it. For this reason, IR viewing cards were used to track the beam path throughout the experiment. Since the power of the laser was high and had the potential for great eye injury, safety glasses were worn at all times of laser operation.

This particular laser was used for multiple experimental setups. For this reason, the laser went through a series of apparati. One of these was an intensity control setup; a half wave plate used with a polarizing beam splitter cube. This gave us the ability to monitor the intensity of the laser light entering the system by keeping only one of the polarizations of the laser while dumping the rest of the laser light. This made it possible to vary the intensity from full power (~45mW) to minimum power (< 1mW). This made the data acquisition much easier later in the experiment. The CCD camera used was much too sensitive to have the laser at full power.

This diode laser produced a beam profile that was not Gaussian, an inconvenience, but not a major problem for this experiment. The laser light would eventual be directed to hit a pinhole, as shown in figure 1 and figure 8. The light hitting the pinhole should be as close to plane waves as possible and the traditionally desired Gaussian beam profile is not a necessity in this situation. For the convenience of changing the location laser light output at anytime, the laser light was sent into a fiber optic cable. The light would travel through the cable, bounce around for a moment, and continue into the experimental set up shown in figure 1. This also proved ideal for our set up, considering that the desired product for this project is to produce a mobile cage system/apparatus that can be placed into a preexisting experimental set up, located in another room, which needs a projected atom trap. A fiber optic cable makes this much easier to place; removing the need to align this set up with a new laser. Now, all one would need to do is dump the laser light into the multi-mode fiber optic cable and into the pinhole diffraction system. The fiber optic cable output laser light with a beam profile that no longer resembled a Gaussian curve, but rather a top hat, or step function of intensity. Figure 9 shows what the beam intensity profile would look like

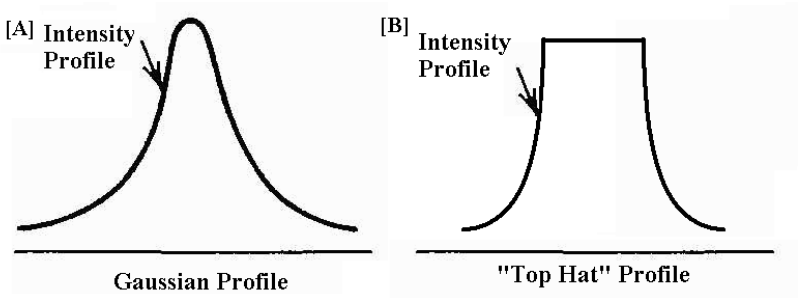

Figure 9. Comparison Between intensity profiles of (A) a Gaussian beam and (B) a "top hat" beam with a more "constant" peak intensity.

compared to a Gaussian beam profile. The beam had a near constant intensity from the edge of the beam to the center of the beam.

3.2 Beam Expander

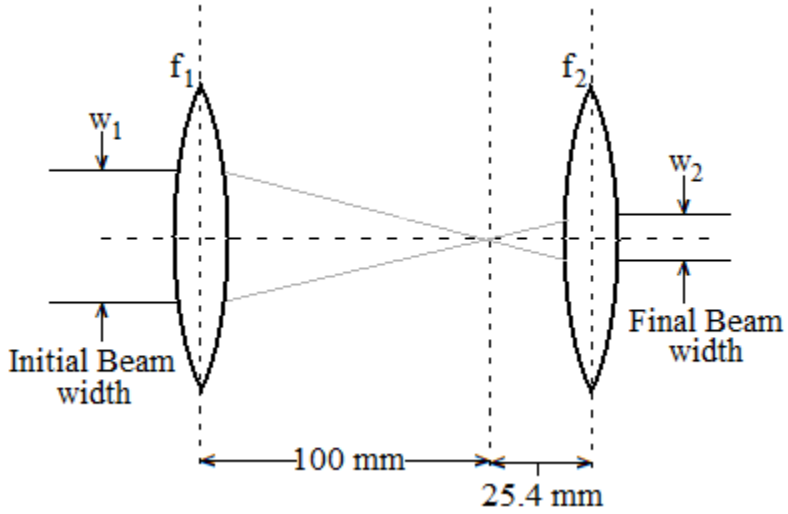

Figure 10. Beam expanding lens system within experimental set up; f_1 = 100 mm and f_2 = 25.4 mm.

The diameter of the beam exiting the cable was around 3-4 mm. Figure 10 shows how a beam expander was used to change the size of the laser beam width for our experiment. The beam expander was used in reverse to shrink the width of the beam. In the case of this system, we had

$$w_2 = \frac{25.4\ mm}{100\ mm} w_1$$

$$w_2 = \frac{1}{4} w_1 = \frac{1}{4}(4mm) = 1 \text{ mm} .$$

Thus, the outgoing beam was ¼ the width of the incoming beam. In this way our ~4 mm beam was shrunk to be a 1 mm beam.

3.3 The Purpose of the Focusing Lens

The focusing lens in this system was 35 mm. The lens needed to be placed a focal length away from the pinhole in order to have the converging wave fronts from the indecent laser light to be plane waves.

3.4 Pinhole placement

Ideally, to duplicate a pseudo-plane wave, one should have the one aperture 3 to 5 times smaller than the beam. The focused light had a spot size of around 300-400 μm, a few times the size of the pinhole itself. The original size of the spot size before it was focused was around 1000 μm (or 1 mm). We can see the saved intensity is actually quite large in this case.

3.5 The Pinhole

In this study the laser light hits a small pinhole (100-μm in diameter) and eventually this forms an interference pattern on a CCD camera. The projection lens is this experiment had a focal length, f = 100 mm. However, if you examine the experimental setup in figure 3 you may notice something strange. The projection lens was placed in front of the pinhole at a nonsensical geometrical distance. Normally when imaging or projecting, a lens is placed a focal length away. In this experiment the projection lens needed to be farther than classical theory would suggest (around 120 or 130 mm in this experiment).

3.6 Pattern Projection

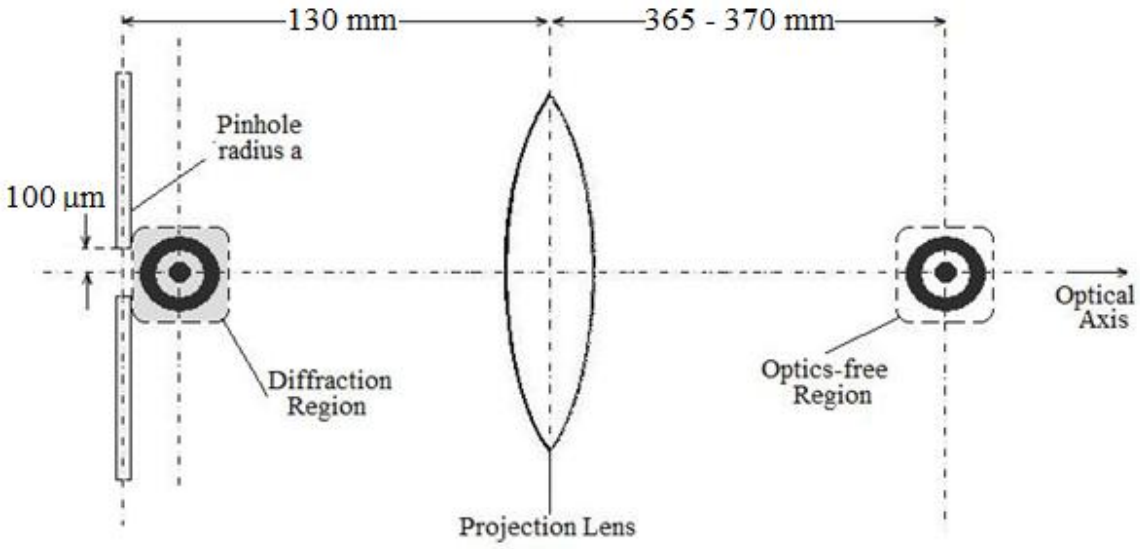

Figure 11. Experimental setup for projecting near-field diffraction patterns to an optics-free region.

The diffraction pattern immediately beyond the 100 μm pinhole was projected by a 100-mm focal length lens to an optics-free region. The optics-free region ranged from 365 mm to 370 mm. Figure 11 shows the experimental setup for the projection lens and pinhole system. The pattern length was slightly larger than 5 mm in its entirety. All the data for each point of interest within the diffraction pattern can be seen in table 1 and figure 13.

The actual values plugged in from figure 7 and equation 3, with n = 2 and λ = 780 nm gives us a representation for f

$$\frac{1}{f} = \frac{1}{\left(130\ mm - \frac{(100\ \mu m)^2}{(2)(780\ nm)}\right)} + \frac{1}{367.94\ mm}$$

$$\frac{1}{f} = 0.010410142\ \text{mm}^{-1}$$

$$f = 96.1\ mm\ ,$$

where f is assume to be 100 mm. This calculation was found using experimentally found values and constants. Here, f was found with a percent error of 4%. This is close enough to the actual value of f for me to trust both equation 3 and the data collected from the

experiment. For two on-axis locations of interest for this experiment, a value of $n = 2$ corresponds to the projection of the primary blue-detuned trap (donut shaped pattern in figure 12A. The data related to the $n = 2$ diffraction pattern can be found in table 1.

4. Data and Analysis

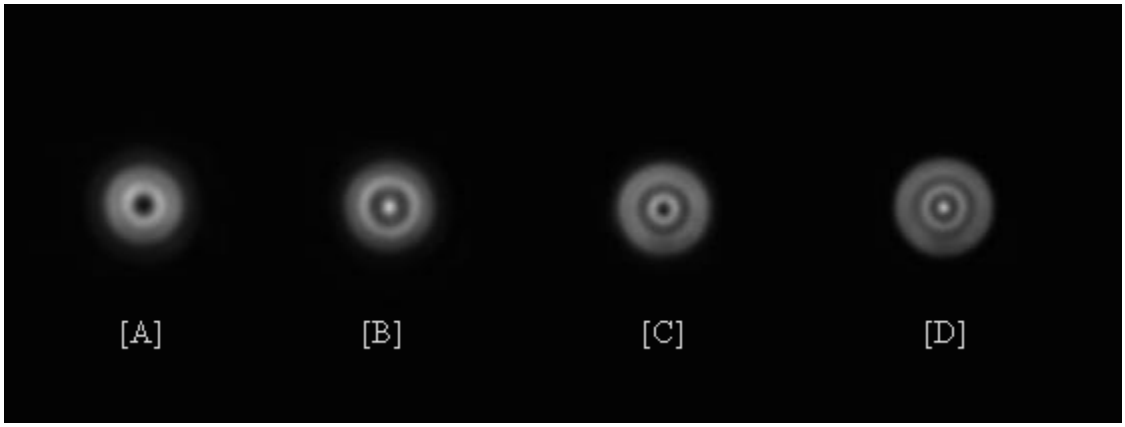

Figure 12. 100-μm pinhole diffraction pattern slices lined up [a] .

Table 1. Pattern Distance (z) of key diffraction pattern points with a lens to pinhole distance of 130 mm.

L (mm)	Pattern #	Pattern Name	Z (mm)
130	1	Initial spot	370.5
130	2	Donut 1	367.94
130	3	Target 1	366.53
130	4	Donut 2	365.15
130	5	Target 2	364.38

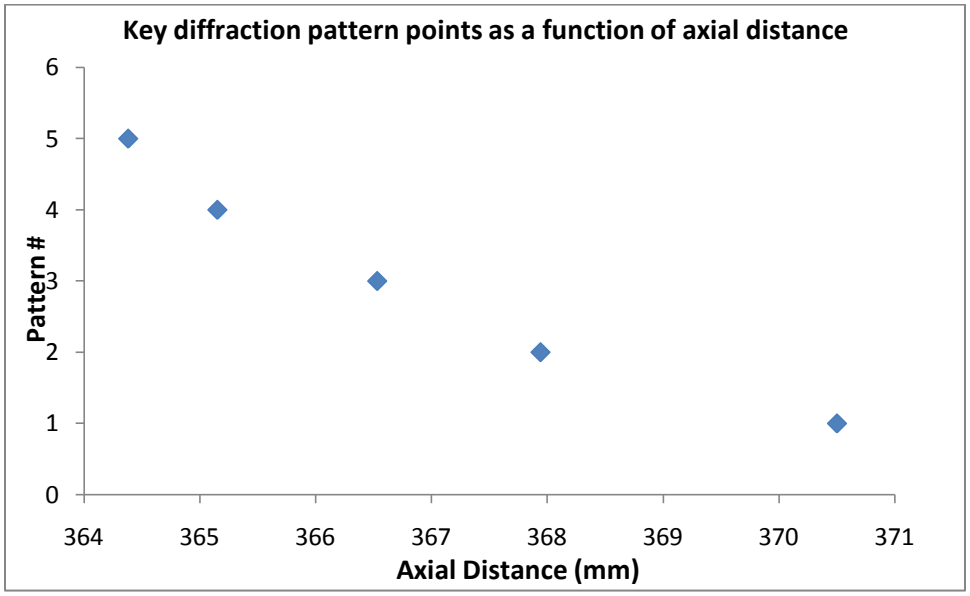

Figure 13. Plot of key diffraction pattern points (2-D slices 1-5) as a function of axial distance

5. Discussion and Conclusion

Actual images for project pinhole diffraction can be seen in figure 11. Images A-D show how the projection pattern changes as a function of axial distance. Table 1 displays the distances each pattern (A-D) was from the projection lens in order to give such an image. The initial spot is not shown in figure 11, however this was the first spot measured, it had no distinct features like the other patterns; it was only a spot.

Figure 13 is graphical representation of the data from table 1. A notable feature of the data can be seen in this form. The distance between the types of diffraction patterns change exponentially. The two types of patterns are target-shaped, red-detuned trap, patterns (figure 11B, 11D) and donut-shaped, blue-detuned trap, patterns figure 11A, 11C). The distance between the donut pattern (11A) and the target pattern (11B) are not equal.

The goal of this study was to create an experimental set up that can observe project pinhole diffraction patterns. Figure 11 is proof that this is possible, and quite effective. The applications of this line of study are nearly limitless, especially in the field of atom trapping. The particular region within the diffraction region that contains the blue-detuned (figure 11A) and red-detuned (figure 11B) trap patterns can each be used as different types of atom traps. What is notable about this experimental set up is that these atom traps have the ability to be projected into optic-free regions which removes the clumsy and crowded equipment and frees up space for other instruments. This projection feature makes these atom traps very useful.

Works Cited

[1] Frank L Pedrotti, Leno S. Pedrotti and Leno M. Pedrotti, *Introduction to Optics*, Third Edition, (Pearson Prentice Hall, Upper Sadler River, NJ, 2007.) pp 267

[2] H. J. Pain, *The Physics of Vibrations and Waves*, Sixth Edition, (John Wiley & Sons Ltd, The Atrium, West Sussex, England, 2005.) pp 376

[3] Amnon Yariv, *Quantum Electronics*, Third Edition, (John Wiley & Sons Inc, Library of Congress Publications, 1989.) pp119, pp122 –use of scanned figures from respective pages.

[4] Katherina Gillen-Christandl, Glen D. Gillen, *Projection of diffraction patterns for use in cold-neutral-atom trapping*, (The American Physical Society, CA, 2010) middle-left of page 3

[5] Katherina Gillen-Christandl, Glen D. Gillen, *Projection of diffraction patterns for use in cold-neutral-atom trapping*, (The American Physical Society, CA, 2010) middle-left of page 4